Low-Temperature Specific Heat of Metallic V-Doped Ti_2O_3 †

M. E. Sjöstrand* and P. H. Keesom
Physics Department, Purdue University, Lafayette, Indiana 47907
(Received 18 September 1972)

The specific heat of titanium sesquioxide, Ti_2O_3, and the mixed system, $Ti_2O_3 + x\%\ V_2O_3$, with x ranging from 1.9 to 10.3 wt% has been measured between 0.4 and 20 K. The Debye temperature at 0 K for pure Ti_2O_3 was found to be 674 K. All the V-doped samples are metallic and exhibit an anomalously large excess heat capacity as compared to that of pure Ti_2O_3. At the lowest temperatures the excess specific heat is linear in temperature and can be extrapolated to the origin. At a relatively low temperature, however, the excess specific heat bends over and becomes practically independent of temperature. The exceptionally large linear term found is of the order 50–80 mJ/mole K and is inversely proportional to the V_2O_3 content. The behavior of the excess heat capacity is attributed to an anomaly in the electronic density of states. The specific heat calculated for an electron gas with a density of states varying according to $E^{-1/2}$ is in good agreement with the experimental results and gives the right concentration dependence for the linear term in the specific heat. The implications of such a model are discussed.

I. INTRODUCTION

During the last decade a substantial experimental and theoretical effort has been expended in understanding the electrical and magnetic properties of titanium sesquioxide, Ti_2O_3. In particular, special attention has been focused on the semiconductor-to-metal transition at 400–600 K which was first reported by Morin.[1] However, prior to that observation, a specific-heat anomaly had been found at 473 K[2] and a later calorimetric study gave similar results with a small anomaly near 453 K.[3]

Recently, several investigations have been extended into the low-temperature region on pure Ti_2O_3 as well as on the mixed system $(V_xTi_{1-x})_2O_3$ for $0 < x < 0.1$. Adding small amounts of V_2O_3 to the Ti_2O_3 host lattice drastically alters its electrical characteristics.[4–6] It also changes its low-temperature thermal properties which will be described in this paper. The addition of V_2O_3 in concentrations over 1 wt% renders the material metallic at all temperatures and for 4–10-wt% V_2O_3 the resistivity is about $5\times10^{-4}\ \Omega$ cm over the whole temperature range.[6] For a V_2O_3 concentration less than about 1 wt%, the temperature dependence of the resistivity still bears some resemblance to semiconducting behavior, but the resistivity at helium temperature is several orders of magnitude lower than that of pure Ti_2O_3.

It has also been found that the conduction is p type,[4] a somewhat surprising observation in virtue of the extra d electron possessed by the vanadium atom as compared to titanium. The state of the V ions in Ti_2O_3 is not well understood but it has been proposed[6] that the p-type conduction might be accounted for if vanadium, directly or indirectly, acts as an electron trap in spite of its excess d electron.

In this paper the specific heat of six samples of $(V_xTi_{1-x})_2O_3$ with x ranging from 0 to 0.103 is presented and discussed. The specific heat of the next-higher oxide of titanium, rutile (TiO_2), was recently investigated in this laboratory,[7] and during the course of this work calorimetric investigations were undertaken elsewhere on several other transition-metal oxides, e.g., V_2O_3 doped with a few wt% Ti_2O_3,[8] V_7O_{13}, and $V_2O_{3.04}$.[9] The specific heat of this class of oxides in the metallic state seems to have one important feature in common, namely, a greatly enhanced linear temperature-dependent term compared to that of ordinary metals. This enhancement effect will be discussed in the latter part of this paper.

II. EXPERIMENTAL

A. Sample Preparation

The single crystals used in this investigation were grown in the Central Crystal Growing Facilities of Purdue University using the Czochralsky–Kyropoulos technique. TiO_2 powder, Ti metal, and V_2O_3,[10] in the proper stoichiometric amounts, were mixed and melted in a molybdenum crucible placed in a resistance-heated Centorr furnace. A detailed description of the crystal-growing procedure is presented elsewhere.[11,12]

Table I gives the notations of the samples together with the corresponding V_2O_3 content in wt% as determined from wet chemical analysis.[13] The accuracy of the analysis is expected to be better than 2% of the V_2O_3 content. However, as only small portions of each boule, usually one piece from the bottom and one from the top, were submitted for analysis, the numbers quoted may reflect some deviation from the true average sample

TABLE I. Sample notations and V_2O_3 content.

Sample No.	114	116	117	118	119	120
wt.% V_2O_3	0.0	3.9	1.9	5.8	8.1	10.3

composition. Two of the samples (Nos. 114 and 120) were also analyzed with respect to residual impurities using mass-spectrographic techniques.[13] In sample No. 114 ("pure" Ti_2O_3) the following impurities were found stated in parts per million by weight (ppmw): C-50, Al-75, Cl-10, K-10, and Fe-13, plus less than 10 ppmw each of N, Mg, Ca, S, V, Cu, Zn, Hf, and Mo. Approximately the same amount of residual impurities was found in sample No. 120. The accuracy of the mass-spectrographic results is moderate but is expected to be better than a factor of 3.

B. Measurement Techniques

All the specific-heat measurements were made using a standard heat-pulse technique in a conventional He^3 cryostat which has been described elsewhere.[14] The addenda included the thermometer, heater wire, glue, etc.; the heat capacity of each commercial Ge resistance thermometer was measured separately and corrections due to the other constituents of the addenda were obtained from published data.

The temperature calibrations were based on the 1958 He^4 scale for T between 1.2 and 4.2 K and on the 1962 He^3 scale for T between 1.2 and 0.4 K. Below 0.4 K the calibration was accomplished by measuring the paramagnetic susceptibility of a sphere of ferric ammonium sulphate granules. A Ge thermometer calibrated by the manufacturer[15] was employed for heat-capacity measurements in the temperature range 4.2–20 K. We estimate that the total systematic error in the measured heat capacity should not be larger than 1–1.5% in the intermediate temperature range ($1 < T < 6$–7 K) but slightly larger at the extreme low temperatures ($T \simeq 0.3$–0.5 K). For T above 7 K the error will increase with temperature and might amount to 5–10% between 15 and 20 K.

III. PURE Ti_2O_3

A. Specific Heat between 0.3 and 20 K: Results and Discussion

As was mentioned in Sec. I, the specific heat of Ti_2O_3 has previously been measured in the high-temperature region where the electrical semiconductor-to-metal transition is observed.[2,3] No results have hitherto been reported on the heat capacity at low temperatures. Since pure Ti_2O_3 below 400–500 K has the properties of a semiconductor with a band gap of 0.02–0.05 eV,[16,17] we should expect that at low temperatures only the phonons will contribute to the heat capacity.

The results of the specific heat C are shown in Fig. 1 in a form in which heat-capacity data are commonly presented, viz., as a plot of C/T vs T^2. For T^2 below 80 K^2 each circle in Fig. 1 represents the average of several data points because of the large number of data taken. From Fig. 1 it is evident that C/T vs T^2 closely follows a

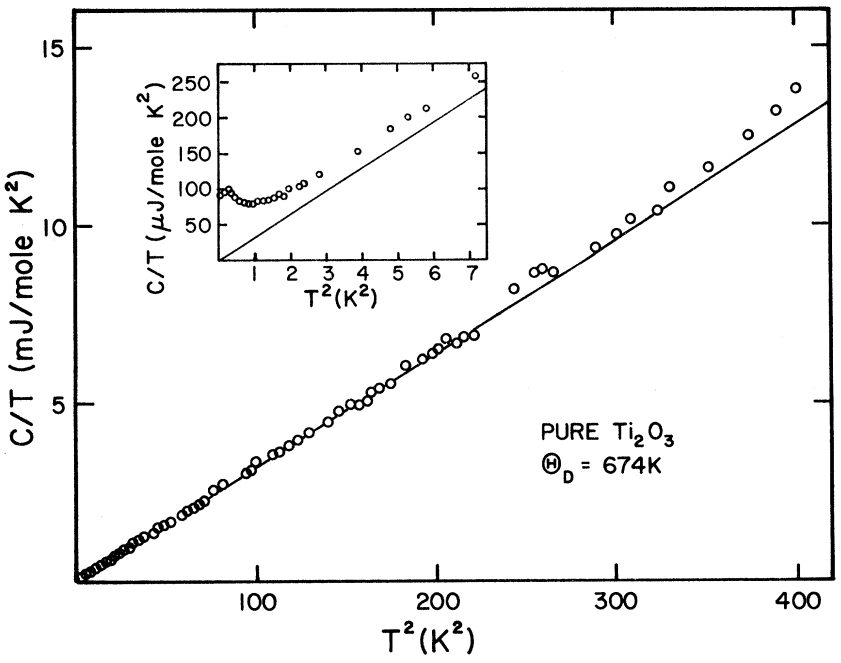

FIG. 1. Specific heat of pure Ti_2O_3 (sample No. 114) plotted as C/T vs T^2. The insert shows a small anomaly in C at the lowest temperatures. The solid line is a linear least-mean-square fit to the experimental data for $3 < T < 15$ K yielding a Debye temperature $\Theta_D = 674$ K.

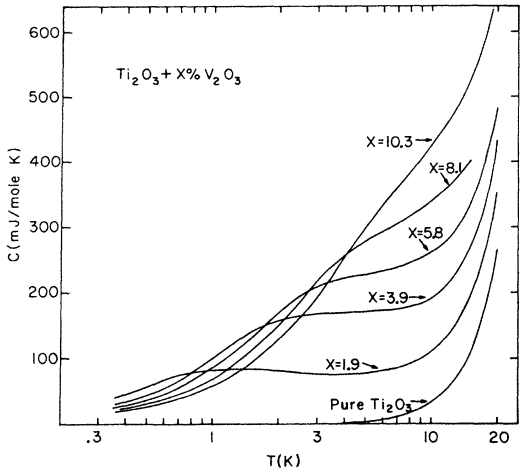

FIG. 2. Specific heat of five metallic samples of $Ti_2O_3 + xV_2O_3$ with x ranging from 1.9 to 10.3 wt%. The heat capacity of pure Ti_2O_3 is also displayed for comparison.

straight line as expected, at least up to 14–15 K. The lattice specific heat C_L in the Debye approximation can be expressed as

$$C_L = 1944n(T/\Theta_D)^3 \text{ J/mole K}, \quad (1)$$

where n is the number of atoms per molecule and Θ_D is the Debye temperature at absolute zero. A least-mean-square fit of C/T vs T^2 in Fig. 1 between 3 and 15 K yields a slope of 31.7 ± 0.3 μJ/mole K^4. With 5 atoms per molecule Ti_2O_3, Θ_D is evaluated from Eq. (1) to be 674 ± 12 K, where the uncertainties include both systematic errors and the spread in the data points. The solid line in Fig. 1 is drawn for $C/T = 31.7T^2$ μJ/mole K^2, and for temperatures above 15 K one observes that the experimental data show a slight positive deviation from this linear relation. However, in this particular temperature region there is a considerable scatter in the data points. Nevertheless, the weak upward curvature is indicative of the onset of the next-higher T^5 term.

The value of $\Theta_D = 674 \pm 12$ K agrees reasonably well with the value of 709 K obtained by Chi and Sladek[18] from measurements of the elastic constants of Ti_2O_3. Probably the difference would be resolved if samples of higher purity become available.

A more detailed examination of the experimental data at the lowest temperatures reveals a small anomaly which is shown in the insert of Fig. 1. This anomaly is likely of Schottky type and has its origin in one (or several) of the residual magnetic ions listed above.

IV. SPECIFIC HEAT OF METALLIC $(V_xTi_{1-x})_2O_3$

A. Results

An overview of the total measured specific heat of five metallic $(V_xTi_{1-x})_2O_3$ samples with a V_2O_3 concentration between 1.9 and 10.3 wt% is presented in Fig. 2 together with the heat capacity of pure Ti_2O_3 for comparison. For clarity we have chosen to present the heat capacity in this graph in the form of smooth curves instead of all the individual data points. In Fig. 2 we notice that all the samples exhibit an anomalously large heat capacity compared to that of pure Ti_2O_3 and that the specific heat has a pronounced plateau in the intermediate temperature region; for increasing V_2O_3 concentration this latter feature gradually disappears. A better qualitative picture of the heat capacity is obtained if instead the excess specific heat (C_{ex}) is plotted rather than the total measured specific heat. The excess specific heat is defined as the difference between the measured specific heat of a vanadium doped sample and that of pure Ti_2O_3. This nomenclature will consistently be used throughout this paper for all the $(V_xTi_{1-x})_2O_3$ samples. Hence, any variation in the lattice specific heat C_L due to the change in the phonon spectrum when vanadium is incorporated in the lattice will be reflected in the excess specific heat. The excess specific heat of sample Nos. 116 and 118 is shown in Fig. 3 and for sample Nos. 119 and 120 in Fig. 4. An overview of the excess specific heat of all the above four samples in the low-temperature region is summarized in Fig. 5.

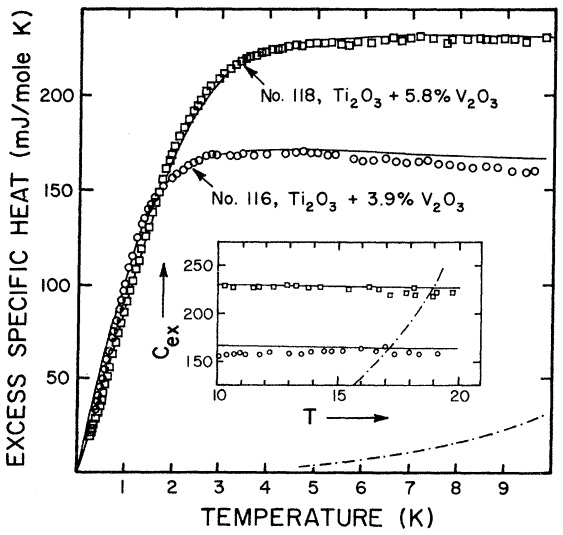

FIG. 3. Excess specific heat of $(V_{0.039}Ti_{0.961})_2O_3$ and $(V_{0.058}Ti_{0.942})_2O_3$ as a function of temperature. The solid curve represents calculated heat capacity as described in text.

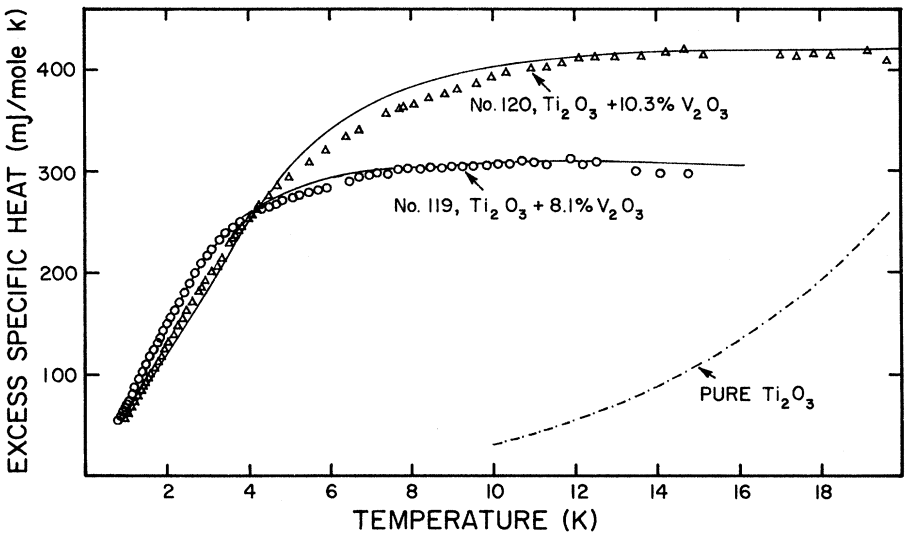

FIG. 4. Excess specific heat of $(V_{0.081}Ti_{0.919})_2O_3$ and $(V_{0.103}Ti_{0.897})_2O_3$ as a function of temperature. The solid curves represent calculated heat capacity as described in text.

The excess specific heat of sample No. 117 which has the lowest V_2O_3 content, 1.9 wt%, is displayed in Fig. 6. This Ti_2O_3-V_2O_3 composition exhibits a small magnetic contribution to the heat capacity in an applied magnetic field of 9 kOe, while on the contrary, in the four other metallic samples no magnetic specific heat could be detected.

All the solid curves in Figs. 3–5 represent calculated heat capacities according to a model which will be described in detail in the subsequent discussion.

A number of important features of the excess specific heat are evident from Figs. 3–5 and are summarized below.

(a) The magnitude of the excess specific heat is unusually large, ranging between 100 and 400 mJ/mole K.

(b) At the lowest temperatures (Fig. 5) the excess specific heat is linear in temperature and can be extrapolated to the origin; the slope of C_{ex} is inversely proportional to the V_2O_3 concentration.

(c) At a temperature which is characteristic for each Ti_2O_3–V_2O_3 composition, the excess specific heat bends over and thereafter remains practically constant to the highest temperature to which the measurements were extended.

(d) The constant value of C_{ex} in the high-temperature region is roughly proportional to the V_2O_3 content.

(e) The heat capacity of all the samples was also measured in an external magnetic field (9 kOe) between 0.4 and 4.2 K (up to 10 K for No. 117) and, except for sample $(V_{0.019}Ti_{0.981})_2O_3$, no difference from the zero-field data could be noticed within the accuracy of the measurements (1–2%). The excess specific heat of $(V_{0.019}Ti_{0.981})_2O_3$, No. 117, is not plotted in Fig. 5 because of its different magnetic behavior. However, as can be seen from Figs. 2 and 6, the general features outlined under (a)–(d) also apply to this sample except that C_{ex} goes through a broad maximum before it attains its constant value. This maximum is enhanced in a magnetic field and simultaneously the temperature of the maximum is displaced to a slightly higher value. The excess magnetic heat capacity gradually levels off to the zero-field specific heat with increasing temperature.

The insert of Fig. 6 shows the excess specific heat of $(V_{0.019}Ti_{0.981})_2O_3$ in the temperature range 5–20 K. At 9–10 K a slight increase of C_{ex} is noticed, but at $T \simeq 13$ K, C_{ex} seems to become constant again. It is not clear whether this behavior of C_{ex} is due to a systematic error in the measure-

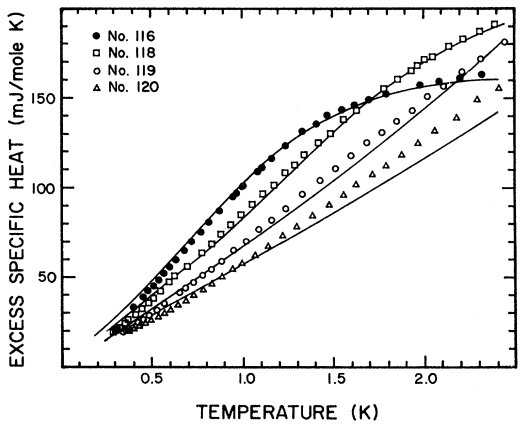

FIG. 5. Excess specific heat of sample Nos. 116, 118, 119, and 120 in the low-temperature region. Solid curves are calculated heat capacity.

ments or if it has its origin in a real effect in the specific heat.

B. Discussion

The metallic character of the alloys suggests that a substantial electronic contribution to the heat capacity should be expected, particularly since the only bands in the vicinity of the Fermi energy are formed primarily by the d orbitals originally associated with the transition-metal ion Ti^{3+}. Furthermore, these d bands can be expected to be very narrow.

A model based on the assumption that the total excess specific heat is electronic in origin will be suggested below and the unexpected behavior of the excess heat capacity will be attributed to an anomaly in the electronic density of states.[19,20] The implications of such a model will be discussed and we will also briefly dwell on alternative possibilities to account for the excess specific heat.

For a degenerate electron gas the heat capacity can be expanded[21] in a power series in T,

$$C_{el} = \tfrac{1}{3}\pi^2 k_B^2 N(E_F)T - \tfrac{1}{6}\pi^4 k_B^4 \{[N'(E_F)]^2/N(E_F) - \tfrac{7}{5}N''(E_F)\}T^3 + \cdots , \quad (2)$$

where $N(E_F)$ is the density of states at the Fermi energy. Ordinarily, experimental data are only analyzed using the first term in Eq. (2). For an isotropic parabolic band, $N(E_F)$ is given by

$$N(E_F) = (4\pi/h^3)(2m^*)^{3/2}(E_F)^{1/2} . \quad (3)$$

The coefficient of T in Eq. (2) is usually denoted by γ and it can easily be shown that

$$\gamma \sim m^*(n_0)^{1/3} , \quad (4)$$

where n_0 is the carrier concentration.

We noticed that the excess specific heat at the lowest temperatures is linear in T and can be extrapolated to the origin which is consistent with the situation in most metals. At a fairly low temperature, however, the excess specific heat bends over and becomes practically independent of temperature. This is a most remarkable feature of the specific heat and within the predictions of a free-electron model this must be interpreted as a transition from a degenerate to a nondegenerate electron gas which has a constant heat capacity $\sim k_B$ per electron in the classical region. The constant value of the heat capacity in the high-temperature region then provides a measure of the carrier concentration n_0 which is approximately directly proportional to the V_2O_3 content. Hence the low-temperature slope γ of C_{ex} is inversely proportional to the carrier concentration which is in direct conflict with what should be expected for a conventional three-dimensional band model where γ is an increasing function of n_0 as given by Eq. (4). Moreover, the magnitude of γ itself is exceptionally large; from Fig. 5 we estimate γ to vary between 50 and 80 mJ/mole K^2 depending on the V_2O_3 content, while γ usually found for pure transition metals ranges between 1 and 10 mJ/mole K^2.

The enhanced γ values cited here for $(V_xTi_{1-x})_2O_3$ would imply for an ordinary isotropic band an extremely narrow bandwidth. Indeed, using a reasonable value for the carrier concentration it can be shown that the bandwidth has to be of the order 0.01 eV. Such a narrow bandwidth would be hard to rationalize with the concept of band states in the ordinary Bloch–Wilson sense.

We will introduce an effective band structure

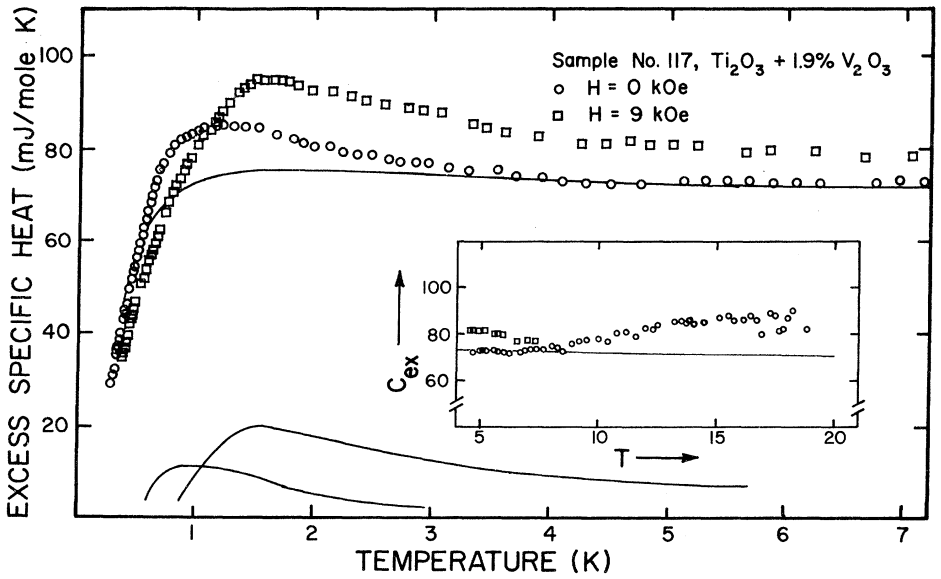

FIG. 6. Excess specific heat of $(V_{0.019}Ti_{0.981})_2O_3$ as a function of temperature in 0 and 9 kOe. The insert shows the high-temperature part of C_{ex}. The upper solid curve represents calculated heat capacity and the two lower curves are the difference between experimental and computed specific heat.

TABLE II. Experimentally determined n_0, T_F, and γ.

Sample No.	wt% V_2O_3	Carriers per mole (10^{22})	T_F (K)	γ $\left(\frac{\text{mJ}}{\text{mole K}^2}\right)$
116	3.9	2.1	5.3	78.0
117	1.9	(1.0)	(2.0)	
118	5.8	2.9	8.5	66.5
119	8.1	3.9	13.5	56.0
120	10.3	5.3	21.5	49.5

which can be approximated by a "one-dimensional" band which in an extreme sense can be described as the electron states formed by the atoms of a linear chain. Although this approach may be too simple, it leads to a surprisingly good agreement between calculated and measured specific heat but it remains to ascertain whether there are physical grounds to support such a hypothesis for this particular compound.

The density of states for a one-dimensional (1D) electron gas takes the form

$$N(E) = [2(2m^*)^{1/2}/h](E)^{-1/2}\,, \tag{5}$$

and γ can be written as

$$\gamma \sim m^*/n_0\,. \tag{6}$$

In view of these two very simple relations we can readily account for the anomalous behavior of the electronic specific heat. The density of states varies in proportion to $E^{-1/2}$ as measured from the band edge, and considering the low carrier concentration (10^{20}–10^{21} cm^{-3}) for this metal, the singularity in $N(E)$ close to the band edge will yield a greatly enhanced γ value as required by the experimental results. Moreover, the experimentally found decrease of γ with increasing V_2O_3 content is reflected in Eq. (6); i.e., for a 1D band, γ is inversely proportional to the carrier concentration n_0. The solid curves in Figs. 3–5 represent the specific heat calculated for an electron gas with a density of states varying according to $E^{-1/2}$ and then fitted to the experimental data by adjusting two parameters, n_0 and the Fermi temperature T_F ($E_F = kT_F$). A method developed by Stoner[22] was employed to derive an explicit expression for the specific heat covering both the degenerate and the classical temperature regions and which for a 1D gas can be written as

$$\frac{C}{nk_B} = \frac{1.5F_{1/2}(\eta)}{F_{-1/2}(\eta)} - 0.25F_{-1/2}(\eta)\left(\frac{dF_{-1/2}(\eta)}{d\eta}\right)^{-1}, \tag{7}$$

where the Fermi integral $F_k(\eta)$ is defined by

$$F_k(\eta) = \int_0^\infty [x^k/(1+e^{x-\eta})]\,dx \tag{8}$$

and $\eta = \mu/k_BT$, where is μ the Fermi energy. η is obtained from the reduced temperature through the relation $T/T_F = 4/[F_{-1/2}(\eta)]^2$. Tabulated values[23] of $F_k(\eta)$ were used in the evaluation of Eq. (7).

The agreement between calculated and experimental heat capacity, as shown in Figs. 3–5, is very satisfactory and in Table II the values of n_0 (carriers per mole) and T_F, as determined by fitting the computed 1D-band heat capacity to the data, are summarized. Also shown in Table II are the γ values as obtained from the initial slope of C_{ex}. The value of T_F for sample No. 117, Ti_2O_3 + 1.9-wt% V_2O_3, is extrapolated and will be clarified later. The magnitude of the unusually large γ leads to a value of 5–8 states of one spin per eV per titantium atom.

The number of carriers per mole is roughly proportional to the V_2O_3 concentration and, on the average, 0.4 carriers are introduced for each V ion. This is in agreement with the carrier densities cited from Hall measurements of $(V_xTi_{1-x})_2O_3$ in Ref. 4.

The degeneracy temperature T_F is for all the samples much smaller than is usually encountered in metals; however, the low T_F is not a consequence of the particular 1D model chosen but follows from the assumption that the total excess specific heat is electronic in origin. For simple metals the Fermi temperature is several orders of magnitude larger than what we have cited here. This huge discrepancy, however, is partly a consequence of the difference in the carrier concentration which is about two to three orders of magnitude smaller in these metallic oxides than in ordinary metals.

In an experimental search for low Fermi temperatures, Junod *et al.*[24] measured the low-temperature heat capacity of a series of compounds of the β-tungsten structure ($A15$), e.g., V_3Si, V_3Ga, etc., and were able to demonstrate the existence of quite low Fermi temperatures (20–40 K). Similar specific-heat measurements on the same class of compounds had previously been done by Bonnerot *et al.*[25] In the $A15$ compounds, A_3B, the A atoms form an array of orthogonal dense linear chains which gives rise to an essential 1D-band structure for the d electrons. Labbé, Friedel, and co-workers[25,26] have been able to give a good description, using a 1D approach, of most of the unusual normal-state properties of the $A15$ compounds. The essential feature of the Labbé–Friedel model is that the Fermi level is adjacent to a high edge in the density-of-states curve, as illustrated in Fig. 7(a) where the density of states for three overlapping d bands is shown. However, as has been pointed out by Cohen *et al.*,[27] this can just as successfully be accounted for by assuming a considerably simpler density-of-states model in the form of an abruptly varying $N(E)$ near the Fermi energy,

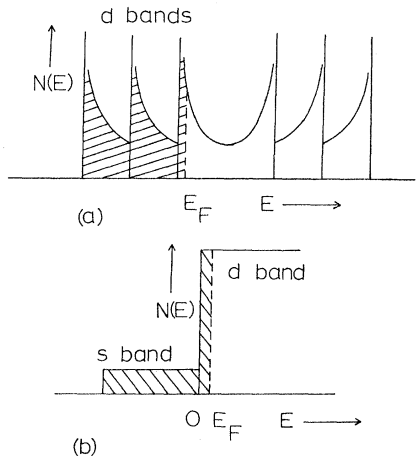

FIG. 7. (a) Schematic representations of the d bands for $A15$ compounds as suggested by Labbé and Friedel. (b) Band model after Cohen *et al.*

$$N(E) = \begin{cases} N_0 , & E \geq 0 \\ \alpha_s N_0 , & E < 0 \end{cases} \tag{9}$$

where α_s is a dimensionless parameter [see Fig. 7(b)]. Physically, the case for $\alpha_s \ll 1$ and $E_F > 0$ corresponds to a situation of a nearly empty d band and an overlapping s band. In view of the results on $(V_xTi_{1-x})_2O_3$ in this investigation, a simplified Cohen density of states would explain the high γ values but it would not account for the decreasing value of γ with increasing Fermi temperature. The latter feature, however, is provided by the Labbé–Friedel model.

During the course of this work, heat-capacity measurements were undertaken on several other metallic transition-metal oxides.[8,9] A common feature of the heat capacity of these metallic oxides seems to be an anomalously enhanced electronic contribution to the specific heat. McWhan and co-workers[8] reported in their investigation of V_2O_3 doped with a few wt.% Ti_2O_3, $(Ti_xV_{1-x})_2O_3$, i.e., the mirror-image compound to the system in this study, an extremely large electronic specific heat yielding a γ value of approximately 80 mJ/K^2 per mole V_2O_3. They interpreted the unusually high γ value as a consequence of a many-body enhancement resulting from strong correlation effects between the electrons in the metallic state of $(Ti_xV_{1-x})_2O_3$. Furthermore, the large electronic specific heat was taken as experimental evidence in support of the model[28] for $(Ti_xV_{1-x})_2O_3$ of a strongly correlated metal approaching a Mott transition.

An explanation of the electronic specific heat of $Ti_2O_3 + xV_2O_3$ on the same physical grounds as described above for $V_2O_3 + xTi_2O_3$ would be difficult to defend if not completely ruled out when considering that the metal-to-semiconductor transition in Ti_2O_3 has none of the qualitative features of a Mott transition.[29]

At this point we should mention two other effects that can contribute to a large electronic γ value. However, neither of them is sufficiently strong to produce the effects which are observed for both $(V_xTi_{1-x})_2O_3$ and $(Ti_xV_{1-x})_2O_3$. The first one is the ordinary electron-phonon interaction which modifies the spectrum of single-particle excitations at the Fermi energy. The enhancement of the band-electron effective mass due to this interaction is, however, very small. The second effect is associated with the interactions of the itinerant carriers with persistent spin fluctuations.[30] The γ enhancement from this type of interaction comes about in much the same way as that due to electron-phonon interaction, i.e., the emission and absorption of spin fluctuations (paramagnons) instead of phonons. The mass enhancement calculated from paramagnon theory[30] is of the order of ten but experimentally the effect was found to be much smaller in, e.g., Ni-Rh alloys.[31] For $(V_xTi_{1-x})_2O_3$ the electron-paramagnon interaction has very little appeal; not only is the enhancement due to this interaction too small but also there is no reason to expect any short-range spin ordering strong enough to produce ferromagnetism at absolute zero as is required by the paramagnon theory.

The experimentally determined n_0 and T_F for sample Nos. 116, 118, 119, and 120 (see Table II) are plotted in Fig. 8 as n_0 vs $(T_F)^{1/2}$. The car-

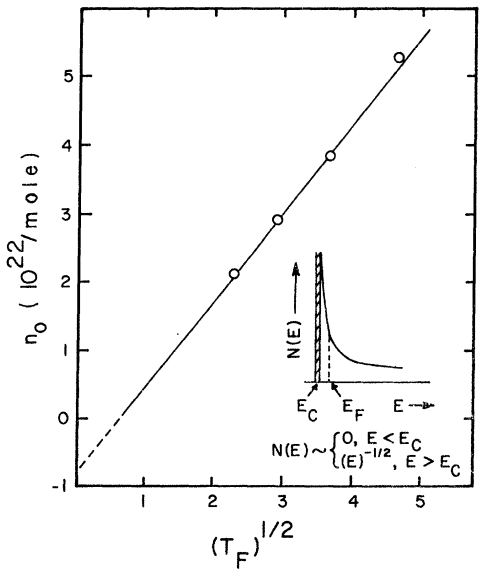

FIG. 8. Number of carriers per mole $(V_xTi_{1-x})_2O_3$ as a function of $(T_F)^{1/2}$. The insert shows a schematic illustration of a one-dimensional density-of-states function.

rier concentration is given by

$$n_0 = \int_0^\infty N(E) f(E)\, dE \,. \tag{10}$$

For a 1D density of states, Eq. (10) is integrated to

$$n_0 = A[(32 m^* k_B)^{1/2}/h](T)^{1/2} \,, \tag{11}$$

with n_0 denoting the number of carriers per mole and A a geometrical constant with dimension of a length. The four data points in Fig. 8 conform closely to a straight line in concordance with Eq. (11). However, we notice that the line has a negative intercept on the ordinate instead of going through the origin. The negative intercept can be interpreted by the following argument. In a real crystal a 1D band is, of course, only a crude approximation to the three-dimensional band structure and particularly the density of states cannot be discontinuous at the band edge. If the $(E)^{-1/2}$ behavior is "cut off" at a suitable low energy to satisfy the condition $N(0) = 0$, which is sketched in the insert of Fig. 8, the negative intercept can be accounted for as to represent the shaded area of "nonavailable states." In this picture the density of states is then

$$N(E) \sim \begin{cases} 0 \,, & E < E_c \\ (E)^{-1/2} \,, & E \geq E_c \end{cases} \tag{12}$$

where we have introduced a cutoff energy E_c. It should be mentioned that the specific heat in Figs. 3–6 was computed without including the cutoff energy. Taking E_c into account leads to computational difficulties in evaluating the heat capacity; however, using a computer routine the specific heat was calculated for the case with a finite cutoff energy E_c. For a reasonable chosen E_c the quantitative effect on the specific heat was small and it certainly did not change the qualitative features of the 1D computed heat capacity and hence this correction was neglected. This correction, however, should be expected to become more significant the smaller the Fermi energy.

Sample No. 117, Ti_2O_3 + 1.9-wt% V_2O_3, constitutes a border case of the metallic $(V_xTi_{1-x})_2O_3$ samples studied in this calorimetric investigation. Its excess specific heat at high temperatures is practically constant, a feature that has been encountered in all the metallic samples, but it exhibits a small broad maximum in the low-temperature region. This maximum is enhanced in a magnetic field and with increasing temperature the enhanced magnetic heat capacity levels off to the zero-field specific heat again. Clearly, paramagnetic ions are present in $(V_{0.019}Ti_{0.981})_2O_3$, but in the alloys with higher V_2O_3 content there is no calorimetric evidence for magnetic ions.

The n_0 vs $(T_F)^{1/2}$ plot in Fig. 8 can be used to deduce the Fermi temperature for sample No. 117 and hence enable us to separate the magnetic contribution to the heat capacity from the electronic contribution. The value of n_0 can be obtained from the constant part of C_{ex} in Fig. 6 and then T_F is estimated from the straight line in Fig. 8. We find $n_0 \approx 1 \times 10^{22}$ carriers per mole and $T_F \approx 2$ K. The upper solid curve in Fig. 6 is the 1D heat capacity calculated with the values of the parameters n_0 and T_F as given above and the two lower curves represent the excess magnetic specific heat obtained by subtracting the computed specific heat from the experimental excess heat capacities. It is apparent that the choice of n_0 and T_F is not perfect; the calculated specific heat seems to be displaced some 0.2–0.4 K towards lower temperatures which results in a negative magnetic heat capacity at the lowest temperatures. This is likely due to the neglect of E_c in calculating C, the effect of which becomes more significant for a lower T_F as was pointed out above. Nevertheless, the qualitative features of the excess magnetic specific heat are apparent: It goes through a maximum and thereafter monotonically decreases to zero. In 9 kOe the height of the maximum is almost doubled and the temperature at which the maximum occurs is displaced to a higher T.

The height of the zero-field curve can be used to get a rough estimate of the concentration of magnetic ions. We find $(0.1–0.3)\times 10^{22}$ ions per mole which is approximately the same amount as has been found in a nonmetallic $(V_xTi_{1-x})_2O_3$ sample ($x = 0.006$) from specific-heat and magnetic-susceptibility measurements.[32]

In the study of the magnetoresistance of Ti_2O_3 with a V_2O_3 content between 0.26–4 wt%,[4] it was concluded that vanadium was magnetically inert in Ti_2O_3 and that the magnetic scattering centers could be attributed to Fe^{3+} in the concentration range 10–100 ppm. This conclusion is hard to rationalize with the present investigation where merely the order of magnitude of the number of paramagnetic ions present indicates that they have to be identified with vanadium and not with trace magnetic impurities in the ppm range. Unfortunately, the highest doped sample in Ref. 4 contained only 3.8-wt% V_2O_3. Therefore no direct comparison can be made between magnetoresistance and the calorimetric observation that no magnetic specific heat could be detected for V_2O_3 $\geq$4 wt%; however, there may still be magnetic ions present in a concentration range (less than 10^{21} centers per mole) which cannot be resolved by specific-heat measurements.

In considering the 1D picture as a possible explanation of the anomalous excess specific heat, the cation d bands in the corundum structure have to be examined in view of a possible band structure that can be approximated by a 1D band. The sym-

metry of the cation d bands in Ti_2O_3 has been elaborated on by Kleiner[33] and a proposed energy-level model which accounts for most of the physical properties of pure Ti_2O_3 was originally put forward by Goodenough.[34] Briefly, the fivefold-degenerate d orbitals of the single electron on Ti^{3+} are split by the combined cubic-trigonal crystalline field (site symmetry C_{3v}) into two e_g orbitals, which are directed toward nearest neighbors in the basal plane, and one a_{1g} orbital directed along the c axis. The trigonal unit cell contains two formula units as there are two sets of molecules which are related by a glidereflection. Hence each cation orbital gives rise to four d-like bands. Furthermore, it is assumed that the a_{1g} states form two doubly degenerate bands which are split as a consequence of the pairing of cations along the c axis; with four electrons per unit cell, one of these bands can be completely filled. Naturally, symmetry does not determine the order in energy of the bands, but by placing an a_{1g} band filled at absolute zero approximately 0.04 eV below the bottom of the higher-lying bands, the semiconducting properties of pure Ti_2O_3 can be accounted for.

It was originally suggested[19] that the lower a_{1g} band alone, which corresponds to wave functions (d_{z^2}) with large lobes directed primarily along the c axis, could approximate the required 1D band without considering the effects of any other overlapping band(s) of different symmetry. The arrays of Ti atoms could then form a set of linear chains which can be treated independently in the Labbé–Friedel picture. The V ions would act as electron traps and thus create the necessary hole carriers in the otherwise filled a_{1g} band.

In comparing the corundum structure with that of V_3Si or other related compounds of $A15$ structure, one has to emphasize one important difference. V_3Si is a body-centered-cubic crystal with respect to Si and the V atoms are located in pairs on each face of the cube so as to form linear chains of V atoms running parallel to the three cubic directions and, moreover, two chains never intersect. Consequently, the 1D hypothesis in V_3Si does not invoke any preferred crystal direction. This, however, is not the case in Ti_2O_3 where for the above model one should expect a much higher carrier mobility along the c direction than compared to that perpendicular to the trigonal axis. To test this, Van Zandt and Eklund[35] measured the resistivity of sample No. 116, $Ti_2O_3 + 3.9$-wt% V_2O_3, both parallel and perpendicular to the c axis in the temperature range 4.2–150 K. The expected large difference in the resistivity did not materialize.

A possible explanation for the absence of the predicted anisotropy in the conductivity could be that the conduction processes are dominated by a relatively small number of carriers from an s band and that the specific heat is governed by the d electrons. Such an assumption would suggest a small overlap between an s band and the manifold of d bands. What argues against this is the fact that the outer s and p orbitals are ordinarily split by a large energy gap between a filled O^{2-} $2p$ band and an empty $4s$ band, with the cluster of d bands located in the middle of the gap several eV from either band edge.

A second explanation for the discrepancy of the resistivity results may be advanced with the following argument. In a real crystal the metal chains are constantly interrupted by different kinds of lattice defects, dislocations, impurities, etc. In a steady current flow the charge carriers have a choice between either overcoming these interruptions directly or jumping to the next adjacent chain. This mechanism may contribute to smear out the difference in conductivity along the c and a directions. However, one may question if it would smear it out so well that the conductivity is practically the same in both crystal directions. Moreover, the conductivity perpendicular to the c axis then ought to be thermally activated which was not apparent from the resistivity results.

To make the resistivity results compatible with the 1D hypothesis one is forced to assume that it is likely that the anomalous band structure cannot be attributed to the a_{1g} band alone but rather that the Fermi energy is located in a vicinity where several d bands of different symmetries overlap and contribute to the electronic density of states. Hence any directional preference of the carrier mobility cannot be distinguished. It has been pointed out before that the role of V in Ti_2O_3 is not well understood; however, it renders the material p type, at least for $V_2O_3 \leq 3.8$ wt%.[4] To what extent the admixture of d-like energy levels of the V ions with the Ti bands effects the density of states at the Fermi energy is not known and cannot be deduced from the specific-heat results, which only yield the electronic density of states at the Fermi level. Further experiments on $(V_xTi_{1-x})_2O_3$ are required to resolve these questions.

V. CONCLUSION

In searching for alternative explanations for the excess specific heat we should recapitulate the definition of C_{ex}. The excess specific heat was defined as the difference between the measured heat capacity of a $(V_xTi_{1-x})_2O_3$ sample and that of pure Ti_2O_3. In the previous discussions we have made the assumption that the lattice specific heat is not significantly altered when V_2O_3 is added even in such a high concentration as 10 wt%. This, we think, is a very plausible assumption in view of the close similarity between host and substitute transition-metal ion. Even if there is a change in

the phonon spectrum between Ti_2O_3 and $(V_xTi_{1-x})_2O_3$ mainly due to the alteration in the lattice parameters,[36,37] this change will only become important at the very highest temperatures, 15–20 K, because of the large magnitude of the excess specific heat. In this temperature range, however, the total systematic error in the measured heat capacity, calibration, etc., also becomes significant as was pointed out in Sec. II and this systematic error is likely to be larger than that introduced by changes in the phonon spectrum.

Another possibility of a modification of the phonon spectrum of Ti_2O_3 when V is added has been considered. The presence of impurities which differ from the atoms of the host lattice in mass or in the interatomic force constants can cause a change in the phonon spectrum in form of low-frequency resonance modes that are localized at the impurity sites.[38] A necessary condition for the existence of these localized phonons, however, is that the substitute atom has a mass, or (and) force constants, appreciably different from that of the host atom, a condition which is not satisfied in the compound $(V_xTi_{1-x})_2O_3$.

A second more hypothetical example of phonon localization is provided by the formation of 1D chains of the substitute atoms and the assumption that these chains are decoupled from the rest of the lattice. Indeed, the specific heat produced by the lattice vibrations of a linear chain of atoms has an initial linear T dependence, but the existence of such linear chains of V atoms not interacting with the Ti_2O_3 host lattice seems to be a rather unlikely physical assumption.

From the above discussion we conclude that an explanation of the specific-heat anomaly in $(V_xTi_{1-x})_2O_3$ is not likely to be found in any change in lattice contribution to the heat capacity but must have its origin somewhere else.

Motional states of ions have been considered as a possible cause for the excess specific heat, e.g., of the kind which are associated with ionic tunneling states.[39] However, this requires that the ions possess a small electric-dipole moment, and furthermore the specific-heat anomaly arising from these excitations is of a Schottky type because of the finite number of tunneling states.

We should emphasize again that the temperature dependence of the excess specific heat is quite different from that of any well-known heat-capacity anomaly, e.g., cooperative λ type, Schottky type, or the broad wedge-shaped specific-heat characteristic of magnetic alloys. Herein lies the great challenge of the problem. Any reasonable physical model that might be able to explain the excess heat capacity has to produce a linear T dependence at the lowest temperatures and a T-independent term at higher temperatures. Moreover, it has to account for the unusual large magnitude of C_{ex} and the inverse V-concentration dependence at the lowest temperatures.

The 1D-band model, albeit for its extreme simplicity, has a great deal of appeal when considering that it accounts for all four of the essential features cited above for the excess specific heat of metallic $(V_xTi_{1-x})_2O_3$.

In the discussion in Sec IV B we have elaborated on several different mechanisms that can result in an enhanced linear term in the specific heat. None of these, however, appear to have a plausible physical ground for being applied to the particular compound $(V_xTi_{1-x})_2O_3$ and the magnitude of enhancement is insufficient to produce the experimentally found γ.

The specific heat of other related metallic transition-metal oxides, $V_2O_3 + xTi_2O_3$,[8] V_7O_3, and $V_3O_{3.04}$,[9] have also yielded unusually large linear temperature-dependent terms with a γ value of approximately the same magnitude as found for $(V_xTi_{1-x})_2O_3$ in this investigation. In the case of $V_2O_3 + xTi_2O_3$ it is not clear if the linear T dependence prevails throughout the total temperature interval ($1 < T < 25$ K) through which the measurements were extended.

Needless to say this raises a very interesting question whether or not the specific-heat anomalies found in $(V_xTi_{1-x})_2O_3$, $(Ti_xV_{1-x})_2O_3$, etc., are of a more general character and might be a characteristic feature of metallic transition-metal oxides. In particular, metallic Ti_2O_3 or V_2O_3 alloyed with small amounts of scandium or chromium would furnish very interesting systems for further calorimetric investigation.

ACKNOWLEDGMENTS

The authors wish to acknowledge Professor L. L. Van Zandt for many informative discussions and also Professor J. M. Honig for his interest and for supplying the crystals.

---

†Work supported by the Advanced Research Projects Agency (IDL Program DAHC-0213) and the National Science Foundation (Project GH34731 and MRL Program GH33574).

*Present address: Physics Department, Brown University, Providence, R. I. 02912.

[1]F. J. Morin, Phys. Rev. Letters 3, 34 (1959).

[2]B. F. Naylor, J. Am. Chem. Soc. 68, 1077 (1946).

[3]S. Nomura, T. Kawakubo, and T. Yanagi, J. Phys. Soc. Japan 16, 706 (1961).

[4]J. M. Honig, L. L. Van Zandt, T. B. Reed, and J. Sohn, Phys. Rev. 182, 863 (1969).

[5]L. L. Van Zandt, J. M. Honig, and J. B. Goodenough, J. Appl. Phys. 39, 594 (1968).

[6]G. V. Chandrashekhar, Q. Won Choi, J. Moyo, and J. M. Honig, Mat. Res. Bull. 5, 999 (1970).
[7]T. R. Sandin and P. H. Keesom, Phys. Rev. 177, 1370 (1969).
[8]D. B. McWhan, J. P. Remeika, T. M. Rice, W. F. Brinkman, J. P. Maita, and A. Menth, Phys. Rev. Letters 27, 941 (1971).
[9]D. B. McWhan, J. P. Remeika, J. P. Maita, H. Okinaka, K. Kosuge, and S. Kachi, Bull. Am. Phys. Soc. 17, 358 (1972).
[10]TiO_2 powder of purity 99.997% was supplied by Johnson Matthey Chemicals Limited, London E. C. 1., England, and Ti metal of purity 99.995% was supplied by Gallard Schlesinger Corp. V_2O_3 was prepared at the Central Crystal Growing Facilities at Purdue University, Lafayette, Ind.
[11]T. B. Reed, R. E. Fahey, and J. M. Honig, Mat. Res. Bull. 2, 561 (1967).
[12]R. E. Loehman, Ph.D. thesis (Purdue University, 1969) (unpublished).
[13]All sample analyses were performed by the Environmental and Materials Characterization Division of the Battelle Memorial Institute, Columbus, Ohio.
[14]G. M. Seidel and P. H. Keesom, Rev. Sci. Instr. 29, 606 (1958).
[15]Manufactured by Cryocal, Inc., Riviera Beach, Fla.
[16]J. Yahia and H. P. R. Frederikse, Phys. Rev. 123, 1257 (1961).
[17]J. M. Honig and T. B. Reed, Phys. Rev. 174, 1020 (1968).
[18]T. C. Chi and R. J. Sladek (unpublished).
[19]M. E. Sjöstrand and P. H. Keesom, Phys. Rev. Letters 27, 1434 (1971).
[20]M. E. Sjöstrand and P. H. Keesom, Phys. Letters 39A, 147 (1972).
[21]E. C. Stoner, Proc. Roy. Soc. (London) A154, 656 (1936).
[22]E. C. Stoner, Phil. Mag. 25, 899 (1936).
[23]A. C. Beer, M. N. Chase, and P. F. Choquard, Helv. Phys. Acta 28, 529 (1955).
[24]A. Junod, J. L. Staudenmann, J. Muller, and P. Spitzli, J. Low Temp. Phys. 5, 25 (1971).
[25]J. Bonnerot, J. Hallais, S. Barišic, and J. Labbé, J. Phys. 30, 701 (1969).
[26]J. Labbé and J. Friedel, J. Phys. 27, 153 (1966); 27, 303 (1966); S. Barišic and J. Labbé, J. Phys. Chem. Solids 28, 2477 (1967).
[27]R. W. Cohen, D. G. Cody, and J. J. Halloran, Phys. Rev. Letters 19, 840 (1967).
[28]D. B. McWhan and J. P. Remeika, Phys. Rev. B 2, 3734 (1970).
[29]N. F. Mott, Phil. Mag. 6, 287 (1961).
[30]J. R. Schrieffer, J. Appl. Phys. 39, 642 (1968).
[31]E. Bucher, W. F. Brinkman, J. P. Maita, and H. J. Williams, Phys. Rev. Letters 18, 1125 (1967).
[32]M. E. Sjöstrand, Ph.D. thesis (Purdue University, 1972) (unpublished).
[33]W. H. Kleiner, MIT Lincoln Lab. Solid State Res. Rept. No. 3, 1967 (unpublished).
[34]J. B. Goodenough, Bull. Soc. Chim. (France) X, 1200 (1965).
[35]L. L. Van Zandt and P. C. Eklund (unpublished).
[36]T. Kawakubo, T. Yanagi, and S. Nomura, J. Phys. Soc. Japan 15, 2102 (1960).
[37]R. E. Loehman, C. N. R. Rao, and J. M. Honig, J. Phys. Chem. 73, 1781 (1969).
[38]A. A. Maradudin, in *Solid State Physics*, edited by F. Seitz and D. Turnbull (Academic, New York, 1966), Vol. 18, p. 273.
[39]V. Narayanamurti and R. O. Pohl, Rev. Mod. Phys. 42, 201 (1970).

PHYSICAL REVIEW B VOLUME 7, NUMBER 8 15 APRIL 1973

Experimental Test of Theories of Extended X-Ray-Absorption-Edge Fine Structure in Metals*

Douglas M. Pease
Institute of Materials Science, University of Connecticut, Storrs, Connecticut 06268
(Received 26 September 1972)

Extended-fine-structure theories may be classified according to whether the final ejected-electron wave function is treated as a spherical or a plane wave. The relative validity of these two approaches is tested by measurements of the *A* and *B* absorption edges in a random solid solution of *A*- and *B*-type atoms. It is found that the first extended-structure peak of the *A* absorption edge occurs at a different energy, relative to the Fermi level, than does the corresponding peak of the *B* absorption edge in the same alloy. The observed energy shifts between *A* and *B* absorption edges agree quantitatively with predictions of spherical-wave theory, whereas such shifts are not predicted to occur by plane-wave theories.

I. INTRODUCTION

There are at present many theories of the extended absorption fine structure (EXAFS) in x-ray absorption spectra,[1–8] but no consensus as to which, if any, of the various theoretical approaches is superior. Azároff concludes, in his first review of the field, that the various theories proposed independently by Kronig,[1] Hayasi,[7] Shiraiwa, Ishimura, and Sawada,[6] Petersen,[3] Kostarev,[2] and